iScience

CellPress
OPEN ACCESS

Article

Targeting extracellular CIRP with an X-aptamer shows therapeutic potential in acute pancreatitis

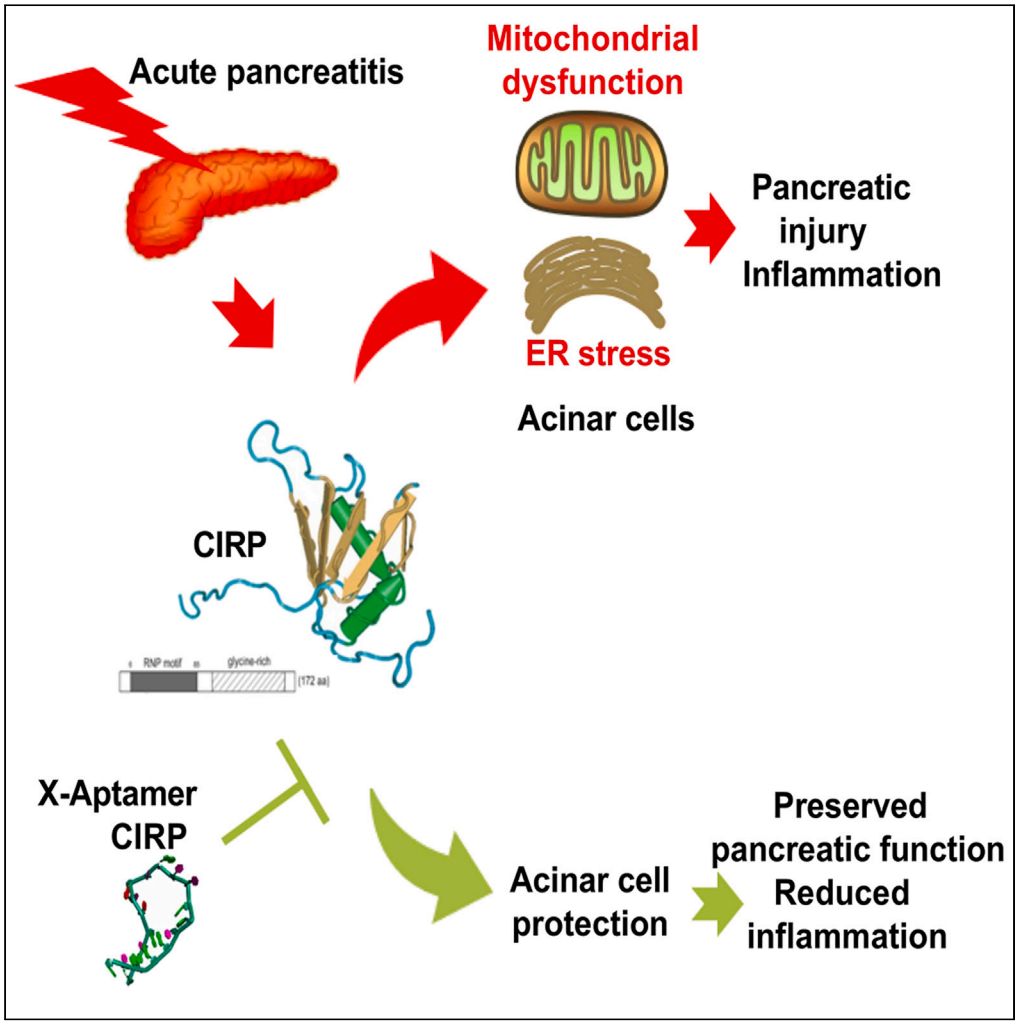

Wuming Liu, Jianbin Bi, Yifan Ren, ..., Yi Lv, Bing Liu, Rongqian Wu

bliu2018@xjtu.edu.cn (B.L.)
rwu001@mail.xjtu.edu.cn (R.W.)

Highlights

Serum CIRP levels are increased in acute pancreatitis (AP)

CIRP deficiency alleviates pancreatic damage and inflammation in AP in mice

Targeting extracellular CIRP with an X-aptamer is protective in experimental AP

Liu et al., iScience 26, 107043
July 21, 2023
https://doi.org/10.1016/j.isci.2023.107043

iScience

CellPress
OPEN ACCESS

Article

Targeting extracellular CIRP with an X-aptamer shows therapeutic potential in acute pancreatitis

Wuming Liu,[1,2] Jianbin Bi,[1,3] Yifan Ren,[1,4] Huan Chen,[5] Jia Zhang,[1,6] Tao Wang,[1,2] Mengzhou Wang,[1,2] Lin Zhang,[1,2] Junzhou Zhao,[1,2] Zheng Wu,[2] Yi Lv,[1,2] Bing Liu,[5,*] and Rongqian Wu[1,7,*]

SUMMARY

Severe acute pancreatitis (AP) is associated with a high mortality rate. Cold-inducible RNA binding protein (CIRP) can be released from cells in inflammatory conditions and extracellular CIRP acts as a damage-associated molecular pattern. This study aims to explore the role of CIRP in the pathogenesis of AP and evaluate the therapeutic potential of targeting extracellular CIRP with X-aptamers. Our results showed that serum CIRP concentrations were significantly increased in AP mice. Recombinant CIRP triggered mitochondrial injury and ER stress in pancreatic acinar cells. $CIRP^{-/-}$ mice suffered less severe pancreatic injury and inflammatory responses. Using a bead-based X-aptamer library, we identified an X-aptamer that specifically binds to CIRP (XA-CIRP). Structurally, XA-CIRP blocked the interaction between CIRP and TLR4. Functionally, it reduced CIRP-induced pancreatic acinar cell injury *in vitro* and L-arginine-induced pancreatic injury and inflammation *in vivo*. Thus, targeting extracellular CIRP with X-aptamers may be a promising strategy to treat AP.

INTRODUCTION

Acute pancreatitis (AP) is a common and potentially lethal inflammatory disease. Despite recent advances in minimally invasive techniques and critical care, there is currently no effective and targeted treatment for AP. Other than management of complications, the treatment of AP is mainly supportive.[1] Patients who develop severe AP still have a high mortality rate. The prognosis largely depends on the development of local and systemic inflammatory response.[2]

Cold-inducible RNA binding protein (CIRP) is an intracellular RNA-chaperone. However, it can be released from cells in inflammatory conditions and extracellular CIRP acts as a damage-associated molecular pattern to promote inflammation.[3] Toll-like receptor 4 (TLR4) is the main receptor for extracellular CIRP.[4] A recent study has revealed that serum CIRP concentrations are increased in AP patients and high serum CIRP concentrations predict poor prognosis in severe AP.[5] Inhibition of CIRP-mediated activation of inflammatory responses has been shown to alleviate organ injury in animal models of AP.[6,7] However, the role of CIRP in the pathogenesis of AP remains largely unknown.

Aptamers are short nucleic acids that can bind onto a specific target molecule with high affinity and specificity. Owing to their small size and unique binding properties, nucleic acid aptamers have emerged as a novel and encouraging class of therapeutics for various indications.[8] X-Aptamers are chemically modified DNA aptamers.[9] The modification on the DNA scaffold with non-DNA functional groups allows X-aptamers to interact with a target molecule more vigorously than traditional DNA aptamers. Blocking extracellular CIRP with antibodies,[3] oligopeptides,[10] or microRNAs[11] has been shown to inhibit inflammation and reduce organ injury under various conditions. However, no attempts have been made to explore the potential of using aptamers to antagonize extracellular CIPR.

The main purpose of this study, therefore, was to explore the role of CIRP in the pathogenesis of AP and evaluate the therapeutic potential of targeting extracellular CIRP with X-aptamers in experimental AP.

[1]National Local Joint Engineering Research Center for Precision Surgery and Regenerative Medicine, Shaanxi Provincial Center for Regenerative Medicine and Surgical Engineering, The First Affiliated Hospital of Xi'an Jiaotong University, Xi'an, China

[2]Department of Hepatobiliary Surgery, The First Affiliated Hospital of Xi'an Jiaotong University, Xi'an, China

[3]Department of Oncology, The Second Affiliated Hospital of Xi'an Jiaotong University, Xi'an, China

[4]Department of General Surgery, The Second Affiliated Hospital of Xi'an Jiaotong University, Xi'an, China

[5]BioBank, The First Affiliated Hospital of Xi'an Jiaotong University, Xi'an, China

[6]Department of Gastroenterology, The Second Affiliated Hospital of Xi'an Jiaotong University, Xi'an, China

[7]Lead contact

*Correspondence: bliu2018@xjtu.edu.cn (B.L.), rwu001@mail.xjtu.edu.cn (R.W.)

https://doi.org/10.1016/j.isci.2023.107043

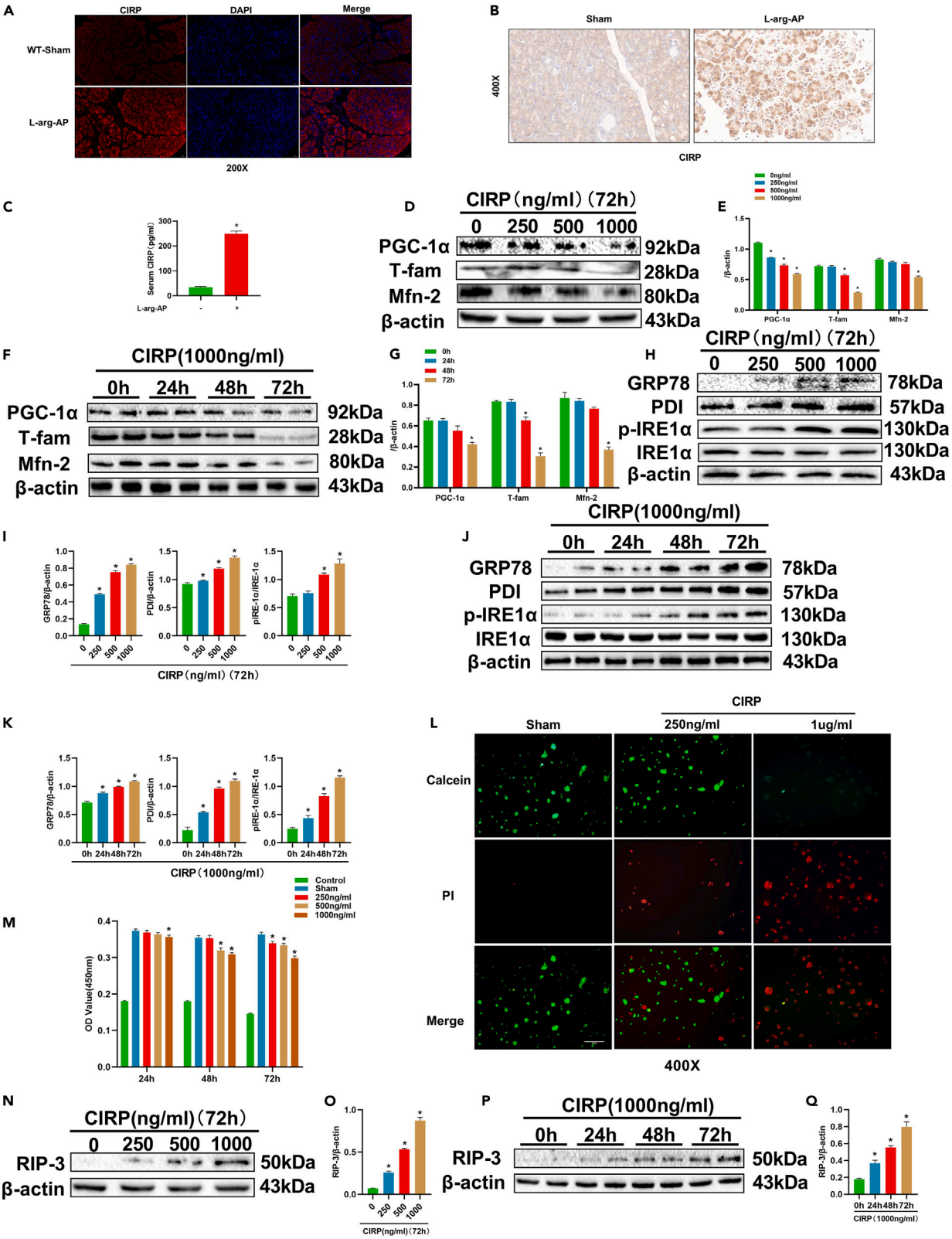
A
CIRP
DAPI
Merge
WT-Sham
L-arg-AP
200X
B
Sham
L-arg-AP
400X
CIRP
C
Serum CIRP (pg/ml)
L-arg-AP
D
CIRP（ng/ml）(72h)
0 250 500 1000
PGC-1α 92kDa
T-fam 28kDa
Mfn-2 80kDa
β-actin 43kDa
E
0ng/ml
250ng/ml
500ng/ml
1000ng/ml
/β-actin
PGC-1α
T-fam
Mfn-2
F
CIRP(1000ng/ml)
0h 24h 48h 72h
PGC-1α 92kDa
T-fam 28kDa
Mfn-2 80kDa
β-actin 43kDa
G
0h
24h
48h
72h
/β-actin
PGC-1α
T-fam
Mfn-2
H
CIRP（ng/ml）(72h)
0 250 500 1000
GRP78 78kDa
PDI 57kDa
p-IRE1α 130kDa
IRE1α 130kDa
β-actin 43kDa
I
GRP78/β-actin
PDI/β-actin
pIRE-1α/IRE-1α
CIRP（ng/ml）(72h)
J
CIRP(1000ng/ml)
0h 24h 48h 72h
GRP78 78kDa
PDI 57kDa
p-IRE1α 130kDa
IRE1α 130kDa
β-actin 43kDa
K
GRP78/β-actin
PDI/β-actin
pIRE-1α/IRE-1α
0h 24h48h72h
CIRP（1000ng/ml）
L
CIRP
Sham
250ng/ml
1ug/ml
Calcein
PI
Merge
400X
M
Control
Sham
250ng/ml
500ng/ml
1000ng/ml
OD Value(450nm)
24h
48h
72h
N
CIRP(ng/ml)(72h)
0 250 500 1000
RIP-3 50kDa
β-actin 43kDa
O
RIP-3/β-actin
CIRP(ng/ml)(72h)
P
CIRP(1000ng/ml)
0h 24h 48h 72h
RIP-3 50kDa
β-actin 43kDa
Q
RIP-3/β-actin
0h 24h48h72h
CIRP（1000ng/ml）

Figure 1. CIRP expression is increased in AP mice and recombination CIRP directly damages pancreatic acinar cells

(A) Pancreatic CIRP immunofluorescence in sham and AP mice (200X). Scale bars:50μm.

(B) Pancreatic CIRP immunohistochemical analysis in sham and AP mice (400X). Scale bars:20μm.

(C) Serum levels of CIRP in sham and AP mice. L-Arginine-AP was induced by two hourly intraperitoneal injections of 4.0 g/kg L-arginine. The animals were sacrificed at 72 h after the first injection of L-arginine. n = 8/group, *p < 0.05 versus sham group.

(D and E) Western blot analysis of PGC-1a, Tfam and Mfn-2 in AR42J cells. The pancreatic AR42J cells (5×10^5/well) were treated with 250, 500, or 1000 ng/mL recombination murine CIRP for 72 h n = 4/group, *p < 0.05 versus 0-ng/mL group.

(F and G) Western blot analysis of PGC-1a, Tfam and Mfn-2 in AR42J cells. The pancreatic AR42J cells (5×10^5/well) were treated with 1000 ng/mL recombination murine CIRP for 24, 48 or 72 h n = 4/group, *p < 0.05 versus 0-h group.

(H and I) Western blot analysis of GRP78, PDI, IRE1α, and pIRE1α in AR42J cells. The pancreatic AR42J cells (5×10^5/well) were treated with 250, 500, or 1000 ng/mL recombination murine CIRP for 72 h. (n = 4/group, *p < 0.05 versus 0-ng/mL group).

(J and K) Western blot analysis of GRP78, PDI, IRE1α, and pIRE1α in AR42J cells. The pancreatic AR42J cells (5×10^5/well) were treated with 1000 ng/mL recombination murine CIRP for 24, 48, or 72 h n = 4/group, *p < 0.05 versus 0-h group. (L) Calcein/PI cell viability/cytotoxicity assay staining of AR42J cells. The pancreatic AR42J cells (5×10^5/well) were treated with 250, or 1000 ng/mL recombination murine CIRP for 72 h. Scale bars:20μm. (M) Cell counting kit-8 assay of AR42J cells. The pancreatic AR42J cells (5×10^3/well) were treated with 250, 500, or 1000 ng/mL recombination murine CIRP for 24, 48 or 72 h n = 8/group, *p < 0.05 versus control group.

(N and O) Western blot analysis of RIP-3 in AR42J cells. The pancreatic AR42J cells (5×10^5/well) were treated with 250, 500, or 1000 ng/mL recombination murine CIRP for 72 h n = 4/group, *p < 0.05 versus 0-ng/mL group.

(P and Q) Western blot analysis of RIP-3 in AR42J cells. The pancreatic AR42J cells (5×10^5/well) were treated with 1000 ng/mL recombination murine CIRP for 24, 48, or 72 h n = 4/group, *p < 0.05 versus 0-h group. Data are expressed as means ± SEM. See also Figures S1 and S2.

RESULTS

CIRP levels are increased in experimental AP and recombinant CIRP directly damages pancreatic acinar cells

First, we verified that L-arginine-induced AP model can indeed cause pancreatic tissue damage and increase of amylase and lipase (supplemental information: Figure S1). To explore the role of CIRP in AP, we measured pancreatic levels of CIRP in the mouse model of L-arginine-induced AP. We found that pancreatic levels of CIRP increased gradually at 24, 48, and 72 h after the induction of AP (supplemental information: Figure S2). As pancreatic injury reaches its maximum level at 72 h after L-arginine injection,[12,13] we measured serum levels of CIRP at 72 h after L-arginine injection. As is it shown, serum level of CIRP increased by 719% at 72 h after the induction of AP (Figure 1C). According to the results of immunofluorescence, the expression of CIRP in the pancreas increased significantly after L-arginine injection (Figure 1A). Similarly, immunohistochemical analysis showed a significant increase in CIRP levels in pancreatic tissue (Figure 1B).

To investigate the direct effects of extracellular CIRP on pancreatic acinar cells, we treated AR42J cells with various doses of recombinant mouse CIRP for up to 72 h. Mitochondrial dysfunction plays an important role in the pathogenesis of AP.[12,14,15] Recombinant CIRP dose- and time-dependently downregulated the expression of peroxisome proliferative activated receptor-γ coactivator 1α (PGC-1α) and mitochondrial transcription factor (Tfam), two important regulators of mitochondrial biogenesis,[16] in AR42J cells. Similarly, mitofusin-2 (Mfn-2), a regulator of mitochondrial fusion and mitophagy,[17] were decreased after recombinant CIRP treatment (Figures 1D–1G).

Mitochondrial dysfunction can result in ER stress.[15] As it is shown, recombinant CIRP significantly increased the expression of glucose-regulated protein 78 (GRP78), protein disulfide isomerase (PDI), and phosphorylated-inositol-requiring enzyme 1α (p-IRE1α), suggesting persistent ER stress after CIRP stimulation in these cells (Figures 1H–1K).

Recombinant CIRP also directly caused death in pancreatic acinar cells. As it is shown, recombinant CIRP dose-dependently increased dead cells (PI positive cells) and decreased living cells (calcein positive cells) (Figure 1L). In the Cell Counting Kit-8 detection, the proliferation of AR42J cells was significantly inhibited by recombinant CIRP (Figure 1M). Consistently, recombinant CIRP also dose- and time-dependently increased RIP-3 levels, a critical regulator of programmed necrosis, in AR42J cells (Figures 1N–1Q).

CIRP deficiency alleviates pancreatic injury and inflammation in AP mice

To confirm the role of CIRP in the pathogenesis of AP, we induced AP by L-arginine injection in CIRP KO mice. As it is shown, CIRP KO mice displayed less severe pancreatic injury after L-arginine injection than WT mice (Figures 2A and 2B). CIRP KO mice also had smaller necrotic areas, lower RIP-3 expression in

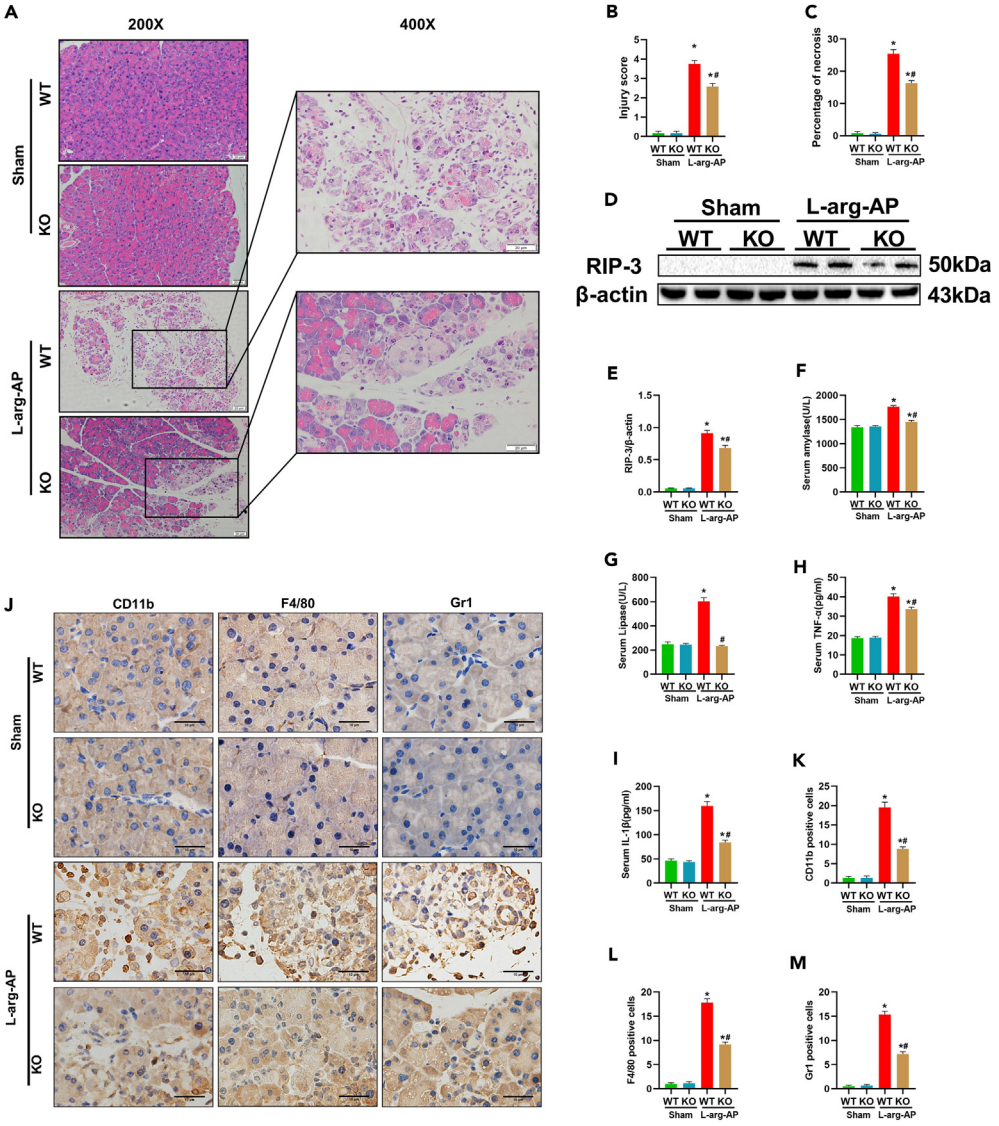

Figure 2. CIRP deficiency alleviates pancreatic injury and inflammation in AP mice

L-Arginine-AP was induced by two hourly intraperitoneal injections of 4.0 g/kg L-arginine in wild type or CIRP knockout mice. The animals were sacrificed at 72 h after the first injection of L-arginine.

(A) Representative photos of hematoxylin and eosin (HE) staining in the pancreas (200X or 400X). Scale bars:20μm.

(B) Pancreatic injury scores.

(C) Percentages of necrotic areas.

(D and E) Western blot analysis of RIP-3 in the pancreas.

(F) Serum amylase levels.

(G) Serum lipase levels.

(H) Serum TNF-α levels.

(I) Serum IL-1β levels.

(J–M) Representative photos and quantitative analysis of F4/80, Gr1, and CD11b staining. Scale bars:10μm.n = 6/group, *p < 0.05 versus sham group; #p < 0.05 versus L-arginine WT group. Data are expressed as means ± SEM.

the pancreatic tissue and lower amylase and lipase levels in the serum than WT mice after L-arginine injection (Figures 2C–2G). The reduced pancreatic injury in CIRP KO mice was associated with lower TNF-α and IL-1β levels in the serum (Figures 2H and 2I) and fewer inflammatory cell infiltration in the pancreatic tissue (Figures 2J–2M) than WT mice.

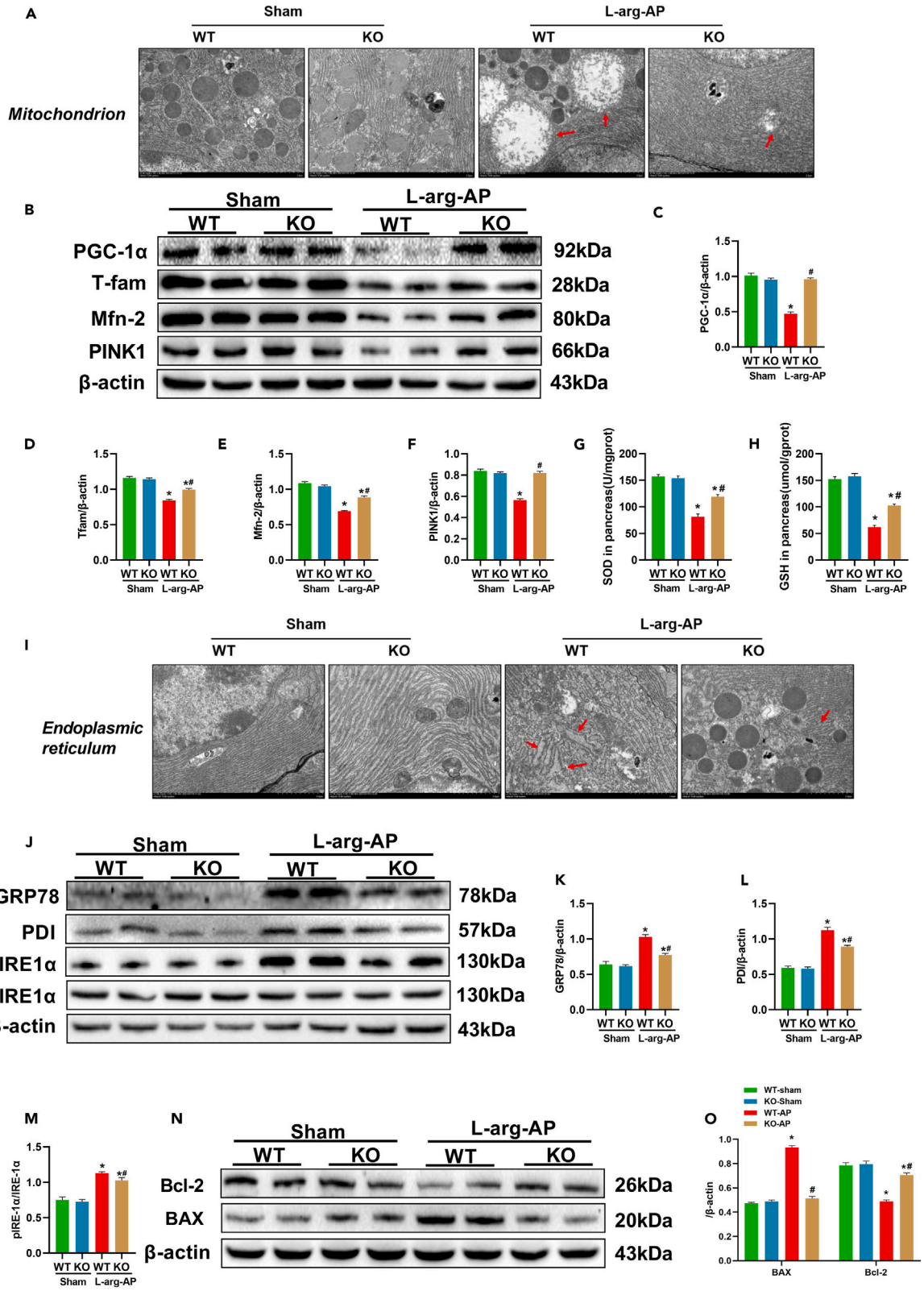
A
Sham
L-arg-AP
WT
KO
WT
KO
Mitochondrion
B
Sham
L-arg-AP
WT
KO
WT
KO
PGC-1α
T-fam
Mfn-2
PINK1
β-actin
92kDa
28kDa
80kDa
66kDa
43kDa
C
PGC-1α/β-actin
WT KO WT KO
Sham L-arg-AP
D
Tfam/β-actin
E
Mfn-2/β-actin
F
PINK1/β-actin
G
SOD in pancreas(U/mgprot)
H
GSH in pancreas(umol/gprot)
I
Sham
L-arg-AP
WT
KO
WT
KO
Endoplasmic reticulum
J
Sham
L-arg-AP
WT
KO
WT
KO
GRP78
PDI
p-IRE1α
IRE1α
β-actin
78kDa
57kDa
130kDa
130kDa
43kDa
K
GRP78/β-actin
L
PDI/β-actin
M
pIRE-1α/IRE-1α
N
Sham
L-arg-AP
WT
KO
WT
KO
Bcl-2
BAX
β-actin
26kDa
20kDa
43kDa
O
WT-sham
KO-Sham
WT-AP
KO-AP
/β-actin
BAX
Bcl-2

Figure 3. CIRP deficiency reduces mitochondrial damage and endoplasmic reticulum stress in AP mice

L-Arginine-AP was induced by two hourly intraperitoneal injections of 4.0 g/kg L-arginine in wild type or CIRP knockout mice. The animals were sacrificed at 72 h after the first injection of L-arginine. (A and I) Ultrastructural alterations in the pancreas (electron microscopy). Scale bars:2μm. (B–F) Western blot analysis of PGC-1a, Tfam, PINK1, and Mfn-2 in the pancreas. (G) The SOD levels in pancreas. (H) The GSH levels in pancreas. (J-M) Western blot analysis of GRP78, PDI, IRE1α, and pIRE1α in the pancreas. (N and O) Western blot analysis of BAX, Bcl-2 in the pancreas; n = 6/group, *p < 0.05 versus sham group; #p < 0.05 versus L-arginine WT group. Data are expressed as means ± SEM.

CIRP deficiency reduces mitochondrial damage and ER stress in AP mice

Consistent with our previous findings,[12,14] electron transmission microscope revealed substantial mitochondrial damage in the pancreatic tissue of WT mice after L-arginine injection. Electron transmission microscope revealed mitochondrial swelling and condensation, disruption, or loss of cristae occurred after the induction of AP in mice. CIRP deficiency appeared to attenuate these pathologic alterations in mitochondrial ultrastructure in AP mice (Figure 3A). In Western blot analysis, L-arginine injection resulted in significant downregulation of several mitochondrial function-related proteins including PGC-1α, Tfam, Mfn-2, and PTEN-induced putative kinase protein 1 (PINK1) in WT mice (Figures 3B–3F). CIRP deficiency prevented L-arginine injection-induced downregulation of PGC-1α, Tfam, Mfn-2, and PINK1 levels in mice. Consistently, L-arginine-induced AP reduced superoxide dismutase (SOD) and glutathione (GSH) levels, which was offset by the CIRP deficiency, suggesting that the CIRP deficiency could significantly ease the level of oxidative stress (Figures 3G and 3H).

Electron transmission microscope also unveiled noticeable swelling and dilation of the ER lumen, suggesting ER stress, in the pancreatic tissue of WT mice after L-arginine injection (Figure 3I). The dilation in the ER lumen was less obvious in CIRP KO mice after L-arginine injection. Western blot analysis showed that CIRP KO mice also had lower levels of ER stress-related proteins including GRP78, PDI, and p-IRE1α than WT mice after the induction of AP (Figures 3J–3M). Excessive endoplasmic reticulum stress can trigger apoptosis. Western blot analysis showed that the level of apoptosis-related protein BAX increased and the level of Bcl-2 decreased in L-arginine injection induced AP mice. In the CIRP KO mice, the effect was significantly reduced (Figures 3N and 3O).

Identification of CIRP targeting X-Aptamers

CIRP targeting X-aptamers were identified from a bead-based X-aptamer library (AM Biotechnologies, Houston, TX, USA) using recombinant human CIRP protein as the target. Eight X-aptamer candidates (supplemental information: Figure S3) were selected for validation of the CIRP antagonizing activity using CIRP-stimulated RAW264.7 cells (supplemental information: Figure S4). The X-aptamer with the strongest CIRP antagonizing activity was used for the subsequent experiments and designated as the XA-CIRP (supplemental information: Figure S3A Sequence 4).

The interaction between CIRP and TLR4 is essential for the pro-inflammatory activity of extracellular CIRP.[3,18,19] Backbone assignment using nuclear magnet resonance (NMR) spectroscopy allows the correlation of residue number with backbone NH cross-peak, which has an important role in biomolecular interaction study. Using standard triple resonance experiment, we fully assigned all possible residues (supplemental information: Figure S5). To verify if CIRP interacts with our screened X-aptamer, we performed NMR titration and isothermal titration calorimetry (ITC) experiments. After unlabeled X-aptamer added to ^{15}N-labeled CIRP, many peaks in the spectrum experience chemical significant peak broadening compared with free CIRP, suggesting the existence of an interaction within intermediate exchange rate regime (Figure 4A). Using ITC, we quantified the affinity of the interaction and calculated the KD as 1.71 ± 0.197 μM (Figure 4B). Then, we assessed the interaction between CIRP and extracellular domain of TLR4 using the NMR and ITC experiments. As shown in (Figures 4C and 4D), CIRP also interacted with extracellular domain of TLR4 with the KD of 3.72 ± 1.98 μM. And importantly, the similar set of amino acids experience peak broadening effect, albeit the difference in the peak intensity change.

Crystal structure of CIRP (PDB ID: 5TBX) shows that CIRP folds into a globular domain. Using the NMR titration for CIRP and X-aptamer, we managed to map the interface on CIRP by highlighting the residues that experienced most significant peak broadening effect (Figure 4E). As the similar set of residues experienced peak broadening effect in the CIRP and TLR4 titration (Figure 4F), residues responsible for CIRP and X-aptamer interaction are also crucial for CIRP and TLR4 interaction. Thus, our screened X-aptamer is a strong competitor of TLR4 for CIRP interaction. As the affinities with CIRP were determined by ITC (Figures 4B and 4D), our screened X-aptamer is a preferred binding partner for CIRP over the extracellular domain of TLR4.

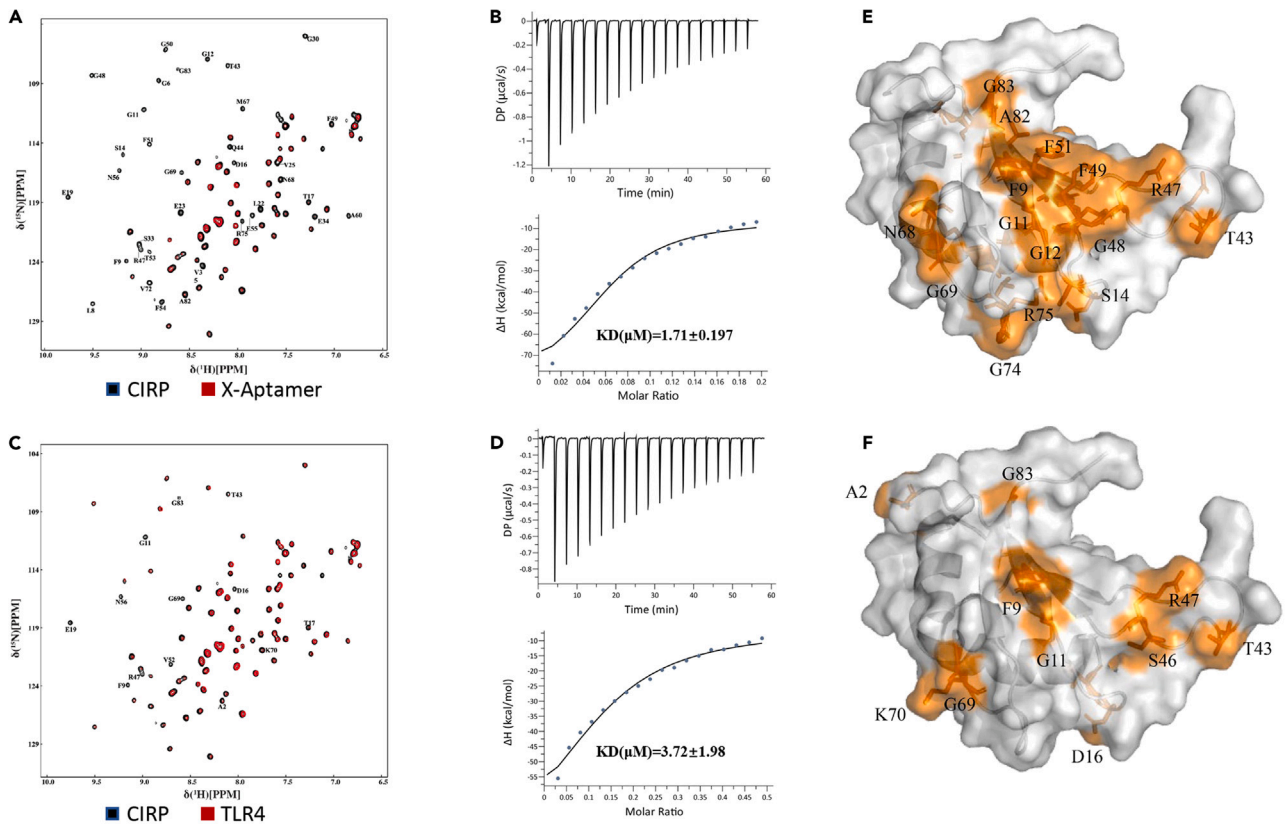

Figure 4. Interaction between CIRP and XA-Aptamers or extracellular domain of TLR4

(A) Overlay of 2D ^{1}H-^{15}N HSQC spectra of the CIRP without (black) and with 5 M equivalents of X-Aptamer (red). The residues experiencing most peak broadening effect are indicated. This characterized peak broadening in the spectrum of the complex indicates intermediate-exchange timescale for NMR or intermediate interaction.

(B) ITC result for CIRP and X-Aptamer. The KD value for the interaction was calculated to be 1.71 μM.

(C) Overlay of 2D ^{1}H-^{15}N HSQC spectra of the CIRP without (black) and with 5 M equivalents of extracellular domain of TLR4 (red). The residues experiencing most peak broadening effect are indicated. This characterized peak broadening in the spectrum of the complex indicates intermediate-exchange or intermediate timescale for NMR interaction.

(D) ITC result for CIRP and extracellular domain of TLR4. The KD value for the interaction was calculated to be 3.72 μM.

(E) The interface for CIRP and X-Aptamer interaction. Orange areas indicate the NMR-derived interface, in which peaks experienced the most broadening effect in NMR titrations.

(F) The interface for CIRP and extracellular domain of TLR4. Orange areas indicate the NMR-derived interface, in which peaks experienced the most broadening effect in NMR titrations. See also Figures S3–S5.

XA-CIRP reduces recombinant mouse CIRP-induced pancreatic acinar cell injury *in vitro*

Immunohistochemical staining of the pancreas showed that the expression of TLR4 was significantly upregulated in the acinar cells of L-arginine-treated mice (supplemental information: Figures S6A and S6B). In addition, recombinant CIRP or caerulein+LPS also increased TLR4 expression in cultured AR42J cells (supplemental information: Figures S6C and S6D).

CIRP is a highly conservative protein. The amino acid sequence of human CIRP is 95.3% identical to mouse CIRP.[20] The XA-CIRP was selected using recombinant human CIRP as the target. To determine whether XA-CIRP can block the activity of mouse CIRP, AR42J cells were treated with either recombinant mouse CIRP or XA-CIRP plus recombinant mouse CIRP. As it is shown, XA-CIRP reduced recombinant mouse CIRP-induced cell death and RIP-3 upregulation in AR42J cells (Figures 5A–5C).

XA-CIRP treatment is protective in experimental AP

To investigate whether the selected XA-CIRP has any beneficial effects in experimental AP, XA-CIRP (10 nmol/kg) was administered intravenously 2 h after the second injection of L-arginine in mice. As shown

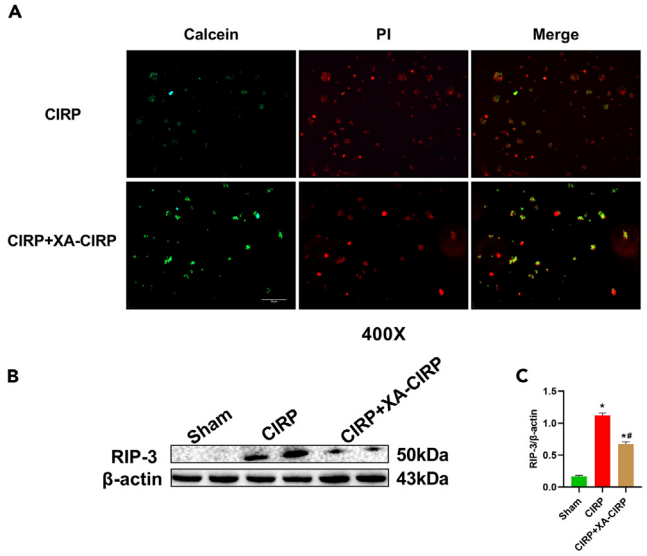

Figure 5. XA-CIRP reduces CIRP-induced pancreatic acinar cell injury *in vitro*

The pancreatic AR42J cells (5×10^5/well) were treated with 1000 ng/mL recombination murine CIRP with or without 1 μM XA-CIRP for 72 h.

(A) Calcein/PI cell viability/cytotoxicity assay staining of AR42J cells. Scale bars:20μm.

(B and C) Western blot analysis of RIP-3. n = 4/group, *p < 0.05 versus sham group, #p < 0.05 versus CIRP group. Data are expressed as means ± SEM. See also Figure S6.

in Figures 6A–6G, XA-CIRP treatment mitigated pancreatic injury, reduced RIP-3 expression and decreased serum levels of amylase and lipase at 72 h after the induction of AP. XA-CIRP treatment also decreased serum levels of TNF-α and IL-1β (Figures 6H and 6I) and inhibited inflammatory cells infiltration (Figures 6J–6M) in experimental AP.

XA-CIRP treatment significantly reduced ultrastructural damage in the mitochondria and ER stress of AP mice (Figures 7A and 7I). Consistently, significantly decreased PGC-1α, Tfam, Mfn-2, and PINK1 levels in the pancreatic tissues of AP mice were also elevated by XA-CIRP treatment (Figures 7B–7F). XA-CIRP treatment also alleviated oxidative stress levels in pancreatic tissue (Figures 7G and 7H). Similarly, significantly increased GRP78, PDI, and p-IRE1α levels in the pancreatic tissues of AP mice were decreased by XA-CIRP treatment (Figures 7J–7M). XA-CIRP treatment can also moderate the level of apoptosis in pancreatic tissue (Figures 7N and 7O).

DISCUSSION

Severe AP remains a serious condition without effective pharmacologic treatment. Here, we show that both serum and pancreatic levels of CIRP were elevated in experimental AP, and CIRP deficiency was protective in mice with AP. Neutralizing CIRP by the X-aptamer XA-CIRP was highly effective in reducing pancreatic injury and inflammation in a mouse model of L-arginine-induced AP. XA-CIRP may meet the urgent medical need for treating AP.

AP is an inflammatory disease. A growing body of evidence has demonstrated that extracellular CIRP is a portent pro-inflammatory mediator.[3,4] It can trigger inflammatory responses via a TLR4-mediated signaling pathway. Directly neutralizing CIRP or inhibiting its activity has been shown to reduce inflammation under various conditions.[3,10,11,21] Serum CIRP levels are elevated in patients with AP.[5,6] CIRP can be released in multiple pathological contexts. Release of CIRP can occur actively from activated macrophages and passively from necrotic cells.[4] As extracellular CIRP can bind to TLR4, theoretically, any cells that expressed TLR4 can be targeted by CIRP. Several studies have suggested that CIRP contributes to the development of inflammation in AP. Linders J et al. revealed that extracellular CIRP is a critical regulator of neutrophil extracellular trap (NET) formation in the inflamed pancreas and targeting extracellular CIRP with the CIRP-derived oligopeptide C23 protects against taurocholate-induced pancreatic injury and inflammation in mice.[6] Xu Q et al. showed that emodin, a natural ingredient of Rhei Radix et Rhizoma (i.e., Da Huang), attenuates severe AP-induced acute lung injury by blocking CIRP-mediated activation of the NLRP3/IL-1β/CXCL1 signaling pathway.[7] Our

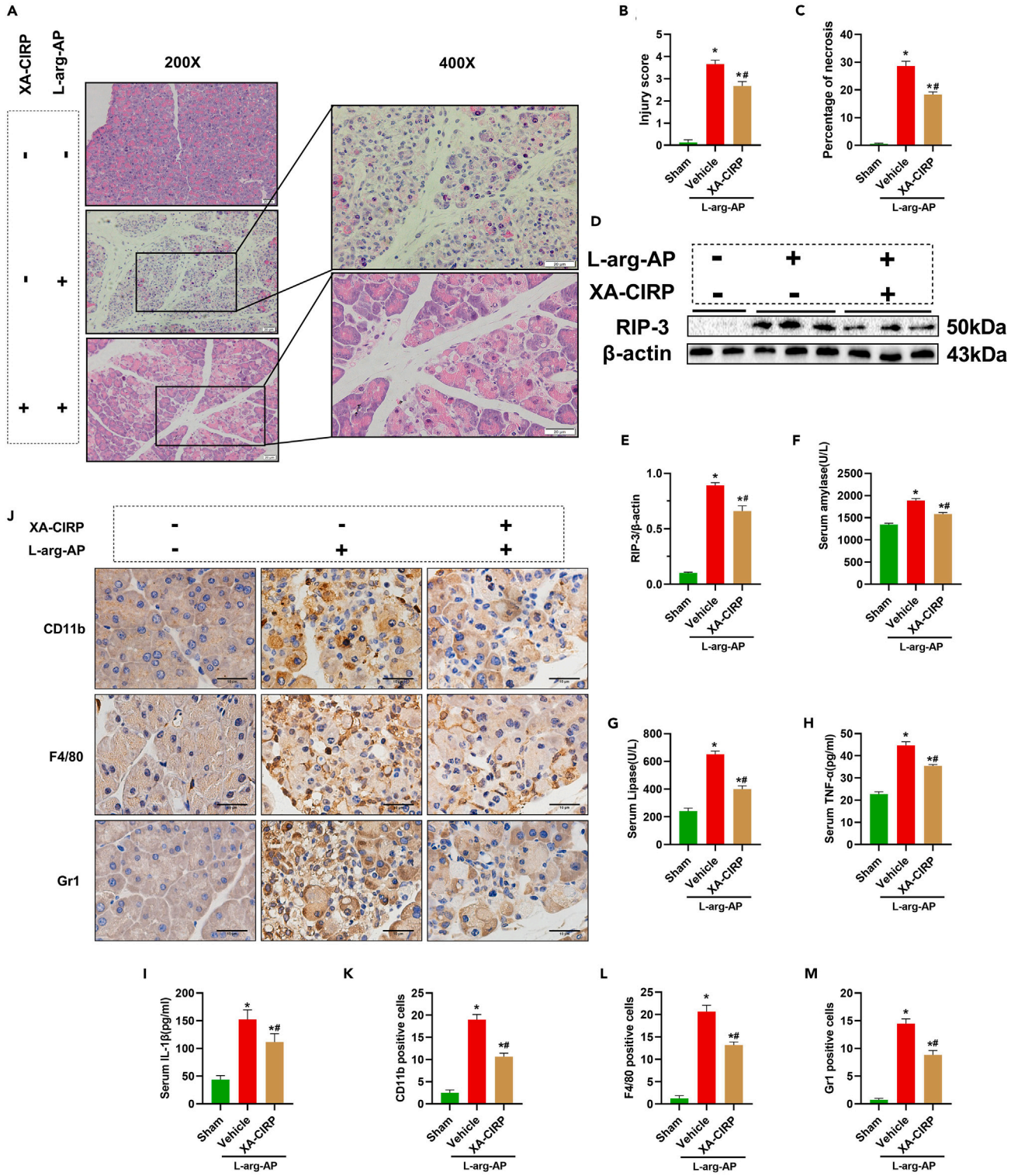

Figure 6. XA-CIRP attenuates pancreatic injury and inflammation in AP mice. L-Arginine-AP was induced by two hourly intraperitoneal injections of 4.0 g/kg L-arginine

At 2 h after the last injection of l-arginine, XA-CIRP (10 nmol/kg BW) or control was administered via the tail vein 2 h after the second injection of L-arginine solution. Blood and pancreatic tissue samples were harvested at 72 h after the first injection of L-arginine (i.e., 69 h after the injection of XA-CIRP).
(A) Representative photos of hematoxylin and eosin (HE) staining in the pancreas (200X or 400X). Scale bars:20μm.

Figure 6. *Continued*
(B) Pancreatic injury scores.
(C) Percentages of necrotic areas.
(D and E) Western blot analysis of RIP-3 in the pancreas.
(F) Serum amylase levels.
(G) Serum lipase levels.
(H) Serum TNF-α levels.
(I) Serum IL-1β levels.
(J–M) Representative photos and quantitative analysis of F4/80, Gr1, and CD11b staining. Scale bars:10μm.n = 6/group, *p < 0.05 versus sham group. #p < 0.05 versus L-arginine vehicle group. Data are expressed as means ± SEM.

current study also showed that blocking CIRP or CIRP deficiency resulted in less severe inflammatory responses in AP mice, which adds another line of evidence supporting the pivotal role of CIRP in initiating inflammation during the development of AP.

In addition to the pro-inflammatory role of CIRP in AP, our results suggest that CIRP may also directly induce mitochondrial damage and ER stress in pancreatic acinar cells. Proper functions of the mitochondria and ER are vital for many physiological roles of the pancreas. Accumulating data from both clinical and experimental studies have established the important role of mitochondrial injury in the pathogenesis of AP.[12,14,22,23] Mitochondria are not only the energetic powerhouses but also crucial synthetic hubs of the cell. Pharmacological disruption of mitochondrial dynamics triggers pancreatitis in various animal models and in patients.[24] Mitochondrial dysfunction leads to impaired energy production and ER stress.[25,26] Excessive ER stress can induce cell death and initiate inflammation.[27] Strategies of maintaining mitochondrial function and inhibiting excessive ER stress are the basis of many treatment approaches of AP.[26,28–31] Several studies have demonstrated that the TLR4 signaling pathway is involved in the regulation of mitochondrial and ER functions.[32–35] The results from the current study showed that TLR4 is expressed in pancreatic acinar cells and increased during AP. Therefore, CIRP is a direct disruptor of mitochondrial and ER functions, and neutralizing CIRP may be a way to maintain cellular homeostasis in AP.

Nucleic acid aptamers are a distinct class of nucleic acid molecules that can specifically bind onto proteins or other cellular targets.[36] Compared with antibodies, nucleic acid aptamers are easier to prepare, less immunogenic, smaller in size, and more efficiently to penetrate tissues. The first aptamer-based treatment, pegaptanib (Macugen), was approved for clinical use by the U.S. Food and Drug Administration in 2004.[37] Since then, aptamers have emerged as an attractive tool for *in vivo* treatment applications. In fact, several aptamers are currently under investigation in various stages of clinical trials.[17,38–42] Even greater efforts are being made in preclinical development of aptamer-based therapeutics.[43–46] However, many nucleic acid aptamers developed using the traditional SELEX process do not meet the requirement for therapeutic applications.[47] X-Aptamers were considered to be the next generation aptamers. Unlike traditional SELEX aptamers, X-aptamers incorporate non-DNA functional groups into the DNA scaffold.[9] The addition of these additional functional groups can result in not only a significant boost against nuclease degradation but also amplified binding affinities,[48] which enables X-aptamers to be superior targeting agents. As an RNA chaperone, CIRP is a natural target for nucleic acid aptamers. Using a bead-based X-aptamer library, we identified an X-aptamer that specifically binds to CIRP (XA-CIRP). Structurally, XA-CIRP blocked the interaction between CIRP and TLR4. Functionally, it reduced CIRP-induced pancreatic acinar cell injury *in vitro* and L-arginine-induced pancreatic injury and inflammation *in vivo*. These findings show the feasibility of developing XA-CIRP as an adjunct for AP treatment. In conclusion, our current study suggests that CIRP is a viable therapeutic target for AP and neutralizing extracellular CIRP with X-aptamer-based adjunctive strategy may be a promising approach to alleviate the severity of AP.

Limitations of the study

There are some limitations in the current study. First, the knockout mice used in this study eliminate not only extracellular but also intracellular CIRP. However, the role of intracellular CIRP may be different from the extracellular CIRP. Therefore, the results obtained from CIRP KO mice need to be interpreted with caution. Second, our multidimensional NMR spectroscopy showed overlays of CIRP and TLR4 with XA-CIRP, suggesting that XA-CIRP might block the interaction between CIRP and TLR4. However, we did not actually confirm the blocking effect of XA-CIRP in CIRP and TLR4 interaction. Third, as a feasibility study, the therapeutic effects of XA-CIRP were observed at 72 h after the induction of AP. The long-term effects of XA-CIRP treatment, including survival, remains to be determined in the applied model of AP. Finally, the dose-depended effects and time-course of XA-CIRP treatment also warrant further investigation.

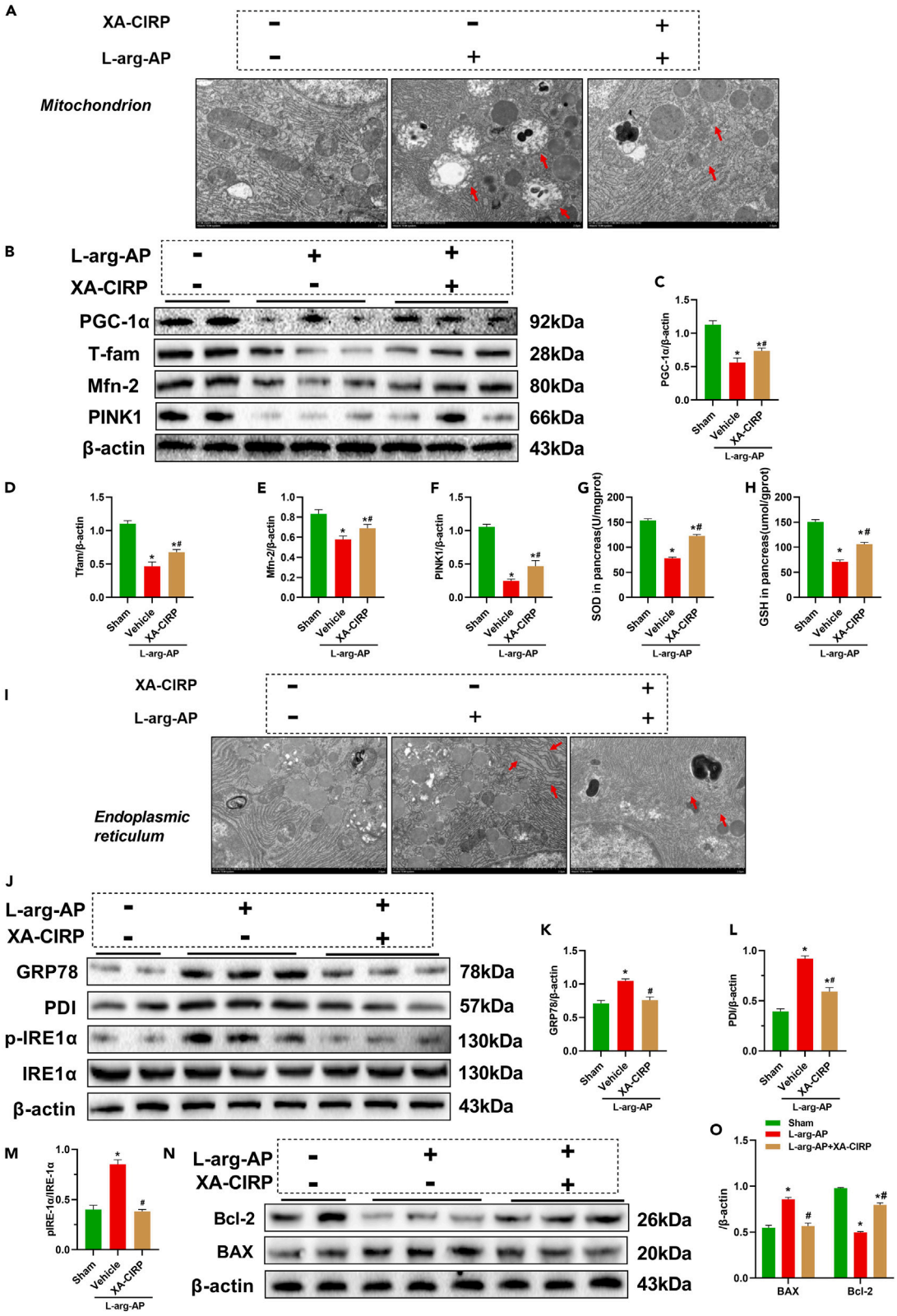
A
XA-CIRP
L-arg-AP
Mitochondrion
B
L-arg-AP
XA-CIRP
PGC-1α
T-fam
Mfn-2
PINK1
β-actin
92kDa
28kDa
80kDa
66kDa
43kDa
C
PGC-1α/β-actin
D
Tfam/β-actin
E
Mfn-2/β-actin
F
PINK1/β-actin
G
SOD in pancreas(U/mgprot)
H
GSH in pancreas(umol/gprot)
Sham
Vehicle
XA-CIRP
L-arg-AP
I
Endoplasmic reticulum
J
GRP78
PDI
p-IRE1α
IRE1α
β-actin
78kDa
57kDa
130kDa
130kDa
43kDa
K
GRP78/β-actin
L
PDI/β-actin
M
pIRE-1α/IRE-1α
N
Bcl-2
BAX
β-actin
26kDa
20kDa
43kDa
O
Sham
L-arg-AP
L-arg-AP+XA-CIRP
/β-actin
BAX
Bcl-2

Figure 7. XA-CIRP can attenuate ER stress and mitochondrial damage in experimental AP mice

L-Arginine-AP was induced by two hourly intraperitoneal injections of 4.0 g/kg L-arginine. At 2 h after the last injection of l-arginine, XA-CIRP (10 nmol/kg BW) or control was administered via the tail vein 2 h after the second injection of L-arginine solution. Blood and pancreatic tissue samples were harvested at 72 h after the first injection of L-arginine (i.e., 69 h after the injection of XA-CIRP).

(A and I) Ultrastructural alterations in the pancreas (electron microscopy). Scale bars:2μm.

(B–F) Western blot analysis of PGC-1a, Tfam, PINK1, and Mfn-2 in the pancreas.

(G) The SOD levels in pancreas.

(H) The GSH levels in pancreas.

(J–M) Western blot analysis of GRP78, PDI, IRE1α, and pIRE1α in the pancreas.

(N and O) Western blot analysis of BAX, Bcl-2 in the pancreas. n = 6/group, *p < 0.05 versus sham group; #p < 0.05 versus L-arginine vehicle group. Data are expressed as means ± SEM.

STAR★METHODS

Detailed methods are provided in the online version of this paper and include the following:

- KEY RESOURCES TABLE
- RESOURCE AVAILABILITY
  - Lead contact
  - Material availability
  - Data and code availability
- EXPERIMENTAL MODEL AND STUDY PARTICIPANT DETAILS
  - Experimental animals and the AP model
  - Cell culture
- METHOD DETAILS
  - Western blot analysis
  - Immunohistochemistry
  - Immunofluorescence
  - Biochemistry detection
  - Histologic evaluation of pancreatic injury
  - Transmission electron microscopy (TEM)
  - Enzyme-linked immunosorbent assay (ELISA)
  - Selection and synthesis of X-Aptamers
  - NMR structure determination
  - Isothermal titration calorimetry (ITC)
  - Administration of XA-CIRP in AP mice
- QUANTIFICATION AND STATISTICAL ANALYSIS

SUPPLEMENTAL INFORMATION

Supplemental information can be found online at https://doi.org/10.1016/j.isci.2023.107043.

ACKNOWLEDGMENTS

We appreciate the administrative support provided by Lirong Yuan, Yan Li, and Juan Zhao during data collection. This work was supported by the National Nature Science Foundation of China (No.82172167 to RW, No. 82100654 to JB and No. 82100685 to YR) and the Innovation Capacity Support Plan of Shaanxi Province grant No.2020TD-040 to RW.

AUTHOR CONTRIBUTIONS

L.W. and B.J. have contributed equally to this work. L.W. acquired and analyzed the data, drafted of the article. R.Y., C.H., Z.J., W.T., W.M., Z.L., Z.J. participated in data acquirement and statistical analysis. W.Z. and L.Y. interpreted the data. L.B. acquired the NMR and ITC data, analyzed the result and revised the paper. W.R. designed and supervised the study and revised the paper. All authors have read and agreed with the final manuscript.

DECLARATION OF INTERESTS

The authors reported no conflict of interest in this study.

INCLUSION AND DIVERSITY

We support inclusive, diverse, and equitable conduct of research.

Received: November 7, 2022
Revised: March 2, 2023
Accepted: June 1, 2023
Published: June 7, 2023

REFERENCES

1. Boxhoorn, L., Voermans, R.P., Bouwense, S.A., Bruno, M.J., Verdonk, R.C., Boermeester, M.A., van Santvoort, H.C., and Besselink, M.G. (2020). Acute pancreatitis. Lancet (London, England) *396*, 726–734. https://doi.org/10.1016/s0140-6736(20)31310-6.

2. Habtezion, A., Gukovskaya, A.S., and Pandol, S.J. (2019). Acute pancreatitis: a multifaceted set of organelle and cellular interactions. Gastroenterology *156*, 1941–1950. https://doi.org/10.1053/j.gastro.2018.11.082.

3. Qiang, X., Yang, W.L., Wu, R., Zhou, M., Jacob, A., Dong, W., Kuncewitch, M., Ji, Y., Yang, H., Wang, H., et al. (2013). Cold-inducible RNA-binding protein (CIRP) triggers inflammatory responses in hemorrhagic shock and sepsis. Nat. Med. *19*, 1489–1495. https://doi.org/10.1038/nm.3368.

4. Aziz, M., Brenner, M., and Wang, P. (2019). Extracellular CIRP (eCIRP) and inflammation. J. Leukoc. Biol. *106*, 133–146. https://doi.org/10.1002/jlb.3mir1118-443r.

5. Gong, J.D., Qi, X.F., Zhang, Y., and Li, H.L. (2017). Increased admission serum cold-inducible RNA-binding protein concentration is associated with prognosis of severe acute pancreatitis. Clin. Chim. Acta *471*, 135–142. https://doi.org/10.1016/j.cca.2017.06.002.

6. Linders, J., Madhi, R., Rahman, M., Mörgelin, M., Regner, S., Brenner, M., Wang, P., and Thorlacius, H. (2020). Extracellular cold-inducible RNA-binding protein regulates neutrophil extracellular trap formation and tissue damage in acute pancreatitis. Lab. Invest. *100*, 1618–1630. https://doi.org/10.1038/s41374-020-0469-5.

7. Xu, Q., Wang, M., Guo, H., Liu, H., Zhang, G., Xu, C., and Chen, H. (2021). Emodin alleviates severe acute pancreatitis-associated acute lung injury by inhibiting the cold-inducible RNA-binding protein (CIRP)-Mediated activation of the NLRP3/IL-1β/CXCL1 signaling. Front. Pharmacol. *12*, 655372. https://doi.org/10.3389/fphar.2021.655372.

8. Shigdar, S., Schrand, B., Giangrande, P.H., and de Franciscis, V. (2021). Aptamers: cutting edge of cancer therapies. Mol. Ther. *29*, 2396–2411. https://doi.org/10.1016/j.ymthe.2021.06.010.

9. Lokesh, G.L., Wang, H., Lam, C.H., Thiviyanathan, V., Ward, N., Gorenstein, D.G., and Volk, D.E. (2017). X-aptamer selection and validation. Methods Mol. Biol. *1632*, 151–174. https://doi.org/10.1007/978-1-4939-7138-1_10.

10. McGinn, J., Zhang, F., Aziz, M., Yang, W.L., Nicastro, J., Coppa, G.F., and Wang, P. (2018). The protective effect of A short peptide derived from cold-inducible RNA-binding protein in renal ischemia-reperfusion injury. Shock *49*, 269–276. https://doi.org/10.1097/shk.0000000000000988.

11. Gurien, S.D., Aziz, M., Jin, H., Wang, H., He, M., Al-Abed, Y., Nicastro, J.M., Coppa, G.F., and Wang, P. (2020). Extracellular microRNA 130b-3p inhibits eCIRP-induced inflammation. EMBO Rep. *21*, e48075. https://doi.org/10.15252/embr.201948075.

12. Ren, Y., Qiu, M., Zhang, J., Bi, J., Wang, M., Hu, L., Du, Z., Li, T., Zhang, L., Wang, Y., et al. (2019). Low serum irisin concentration is associated with poor outcomes in patients with acute pancreatitis, and irisin administration protects against experimental acute pancreatitis. Antioxidants Redox Signal. *31*, 771–785. https://doi.org/10.1089/ars.2019.7731.

13. Kui, B., Balla, Z., Vasas, B., Végh, E.T., Pallagi, P., Kormányos, E.S., Venglovecz, V., Iványi, B., Takács, T., Hegyi, P., and Rakonczay, Z., Jr. (2015). New insights into the methodology of L-arginine-induced acute pancreatitis. PLoS One *10*, e0117588. https://doi.org/10.1371/journal.pone.0117588.

14. Ren, Y., Liu, W., Zhang, L., Zhang, J., Bi, J., Wang, T., Wang, M., Du, Z., Wang, Y., Zhang, L., et al. (2021). Milk fat globule EGF factor 8 restores mitochondrial function via integrin-medicated activation of the FAK-STAT3 signaling pathway in acute pancreatitis. Clin. Transl. Med. *11*, e295. https://doi.org/10.1002/ctm2.295.

15. Biczo, G., Vegh, E.T., Shalbueva, N., Mareninova, O.A., Elperin, J., Lotshaw, E., Gretler, S., Lugea, A., Malla, S.R., Dawson, D., et al. (2018). Mitochondrial dysfunction, through impaired autophagy, leads to endoplasmic reticulum stress, deregulated lipid metabolism, and pancreatitis in animal models. Gastroenterology *154*, 689–703. https://doi.org/10.1053/j.gastro.2017.10.012.

16. Jiang, S., Teague, A.M., Tryggestad, J.B., and Chernausek, S.D. (2017). Role of microRNA-130b in placental PGC-1α/TFAM mitochondrial biogenesis pathway. Biochem. Biophys. Res. Commun. *487*, 607–612. https://doi.org/10.1016/j.bbrc.2017.04.099.

17. Arzamendi, D., Dandachli, F., Théorêt, J.F., Ducrocq, G., Chan, M., Mourad, W., Gilbert, J.C., Schaub, R.G., Tanguay, J.F., and Merhi, Y. (2011). An anti-von Willebrand factor aptamer reduces platelet adhesion among patients receiving aspirin and clopidogrel in an ex vivo shear-induced arterial thrombosis. Clin. Appl. Thromb. Hemost. *17*, E70–E78. https://doi.org/10.1177/1076029610384114.

18. Bolourani, S., Sari, E., Brenner, M., and Wang, P. (2021). Extracellular CIRP induces an inflammatory phenotype in pulmonary fibroblasts via TLR4. Front. Immunol. *12*, 721970. https://doi.org/10.3389/fimmu.2021.721970.

19. Chen, K., Cagliani, J., Aziz, M., Tan, C., Brenner, M., and Wang, P. (2021). Extracellular CIRP activates STING to exacerbate hemorrhagic shock. JCI insight *6*, e143715. https://doi.org/10.1172/jci.insight.143715.

20. Nishiyama, H., Higashitsuji, H., Yokoi, H., Itoh, K., Danno, S., Matsuda, T., and Fujita, J. (1997). Cloning and characterization of human CIRP (cold-inducible RNA-binding protein) cDNA and chromosomal assignment of the gene. Gene *204*, 115–120. https://doi.org/10.1016/s0378-1119(97)00530-1.

21. Zhang, Y., Zhang, J., Ren, Y., Li, T., Bi, J., Du, Z., and Wu, R. (2021). Luteolin suppresses sepsis-induced cold-inducible RNA-binding protein production and lung injury in neonatal mice. Shock *55*, 268–273. https://doi.org/10.1097/shk.0000000000001624.

22. Tran, Q.T., Tran, V.H., Sendler, M., Doller, J., Wiese, M., Bolsmann, R., Wilden, A., Glaubitz, J., Modenbach, J.M., Thiel, F.G., et al. (2021). Role of bile acids and bile salts in acute pancreatitis: from the experimental to clinical studies. Pancreas *50*, 3–11. https://doi.org/10.1097/mpa.0000000000001706.

23. Maléth, J., Hegyi, P., Rakonczay, Z., Jr., and Venglovecz, V. (2015). Breakdown of bioenergetics evoked by mitochondrial damage in acute pancreatitis: mechanisms and consequences. Pancreatology *15*, S18–S22. https://doi.org/10.1016/j.pan.2015.06.002.

24. Debray, F.G., Drouin, E., Herzog, D., Lortie, A., Lambert, M., Garel, L., Mitchell, G.A., and Michaud, J.L. (2006). Recurrent pancreatitis in mitochondrial cytopathy. Am. J. Med. Genet. *140*, 2330–2335. https://doi.org/10.1002/ajmg.a.31457.

25. Bi, J., Zhang, J., Ren, Y., Du, Z., Li, Q., Wang, Y., Wei, S., Yang, L., Zhang, J., Liu, C., et al. (2019). Irisin alleviates liver ischemia-reperfusion injury by inhibiting excessive mitochondrial fission, promoting mitochondrial biogenesis and decreasing

oxidative stress. Redox Biol. *20*, 296–306. https://doi.org/10.1016/j.redox.2018.10.019.

26. Ren, Y., Cui, Q., Zhang, J., Liu, W., Xu, M., Lv, Y., Wu, Z., Zhang, Y., and Wu, R. (2021). Milk fat globule-EGF factor 8 alleviates pancreatic fibrosis by inhibiting ER stress-induced chaperone-mediated autophagy in mice. Front. Pharmacol. *12*, 707259. https://doi.org/10.3389/fphar.2021.707259.

27. Borrello, M.T., Martin, M.B., and Pin, C.L. (2022). The unfolded protein response: an emerging therapeutic target for pancreatitis and pancreatic ductal adenocarcinoma. Pancreatology *22*, 148–159. https://doi.org/10.1016/j.pan.2021.10.007.

28. Ren, Y.F., Wang, M.Z., Bi, J.B., Zhang, J., Zhang, L., Liu, W.M., Wei, S.S., Lv, Y., Wu, Z., and Wu, R.Q. (2019). Irisin attenuates intestinal injury, oxidative and endoplasmic reticulum stress in mice with L-arginine-induced acute pancreatitis. World J. Gastroenterol. *25*, 6653–6667. https://doi.org/10.3748/wjg.v25.i45.6653.

29. Yuan, J., Wei, Z., Xin, G., Liu, X., Zhou, Z., Zhang, Y., Yu, X., Wan, C., Chen, Q., Zhao, W., et al. (2021). Vitamin B(12) attenuates acute pancreatitis by suppressing oxidative stress and improving mitochondria dysfunction via CBS/SIRT1 pathway. Oxid. Med. Cell. Longev. *2021*, 7936316. https://doi.org/10.1155/2021/7936316.

30. Luo, Z.L., Sun, H.Y., Wu, X.B., Cheng, L., and Ren, J.D. (2021). Epigallocatechin-3-gallate attenuates acute pancreatitis induced lung injury by targeting mitochondrial reactive oxygen species triggered NLRP3 inflammasome activation. Food Funct. *12*, 5658–5667. https://doi.org/10.1039/d1fo01154e.

31. Yao, L., Cheng, C., Yang, X., Han, C., Du, D., Liu, T., Chvanov, M., Windsor, J., Sutton, R., Huang, W., and Xia, Q. (2019). Ethyl pyruvate and analogs as potential treatments for acute pancreatitis: a review of in vitro and in vivo studies. Pancreatology *19*, 209–216. https://doi.org/10.1016/j.pan.2018.12.007.

32. Winter, J., Hammer, E., Heger, J., Schultheiss, H.P., Rauch, U., Landmesser, U., and Dörner, A. (2019). Adenine nucleotide translocase 1 expression is coupled to the HSP27-mediated TLR4 signaling in cardiomyocytes. Cells *8*, e121588. https://doi.org/10.3390/cells8121588.

33. Wang, X., Yao, W., Wang, M., Zhu, J., and Xia, L. (2022). TLR4-SIRT3 mechanism modulates mitochondrial and redox homeostasis and promotes EPCs recruitment and survival. Oxid. Med. Cell. Longev. *2022*, 1282362. https://doi.org/10.1155/2022/1282362.

34. Hu, T., Zhao, Y., Long, Y., Ma, X., Zeng, Y., Wu, W., Deng, C., Li, M., Peng, S., Yang, H., et al. (2022). TLR4 promoted endoplasmic reticulum stress induced inflammatory bowel disease via the activation of p38 MAPK pathway. Biosci. Rep. *42*. https://doi.org/10.1042/bsr20220307.

35. Gan, L.T., Van Rooyen, D.M., Koina, M.E., McCuskey, R.S., Teoh, N.C., and Farrell, G.C. (2014). Hepatocyte free cholesterol lipotoxicity results from JNK1-mediated mitochondrial injury and is HMGB1 and TLR4-dependent. J. Hepatol. *61*, 1376–1384. https://doi.org/10.1016/j.jhep.2014.07.024.

36. Blind, M., and Blank, M. (2015). Aptamer selection technology and recent advances. Molecular therapy. Nucleic acids *4*, e223. https://doi.org/10.1038/mtna.2014.74.

37. Gragoudas, E.S., Adamis, A.P., Cunningham, E.T., Jr., Feinsod, M., and Guyer, D.R.; VEGF Inhibition Study in Ocular Neovascularization Clinical Trial Group (2004). Pegaptanib for neovascular age-related macular degeneration. N. Engl. J. Med. *351*, 2805–2816. https://doi.org/10.1056/NEJMoa042760.

38. Choi, S., Han, J., Kim, J.H., Kim, A.R., Kim, S.H., Lee, W., Yoon, M.Y., Kim, G., and Kim, Y.S. (2020). Advances in dermatology using DNA aptamer "Aptamin C" innovation: oxidative stress prevention and effect maximization of vitamin C through antioxidation. J. Cosmet. Dermatol. *19*, 970–976. https://doi.org/10.1111/jocd.13081.

39. Rosenberg, J.E., Bambury, R.M., Van Allen, E.M., Drabkin, H.A., Lara, P.N., Jr., Harzstark, A.L., Wagle, N., Figlin, R.A., Smith, G.W., Garraway, L.A., et al. (2014). A phase II trial of AS1411 (a novel nucleolin-targeted DNA aptamer) in metastatic renal cell carcinoma. Invest. New Drugs *32*, 178–187. https://doi.org/10.1007/s10637-013-0045-6.

40. Jilma-Stohlawetz, P., Gilbert, J.C., Gorczyca, M.E., Knöbl, P., and Jilma, B. (2011). A dose ranging phase I/II trial of the von Willebrand factor inhibiting aptamer ARC1779 in patients with congenital thrombotic thrombocytopenic purpura. Thromb. Haemostasis *106*, 539–547. https://doi.org/10.1160/th11-02-0069.

41. Jilma, B., Paulinska, P., Jilma-Stohlawetz, P., Gilbert, J.C., Hutabarat, R., and Knöbl, P. (2010). A randomised pilot trial of the anti-von Willebrand factor aptamer ARC1779 in patients with type 2b von Willebrand disease. Thromb. Haemostasis *104*, 563–570. https://doi.org/10.1160/th10-01-0027.

42. Gilbert, J.C., DeFeo-Fraulini, T., Hutabarat, R.M., Horvath, C.J., Merlino, P.G., Marsh, H.N., Healy, J.M., Boufakhreddine, S., Holohan, T.V., and Schaub, R.G. (2007). First-in-human evaluation of anti von Willebrand factor therapeutic aptamer ARC1779 in healthy volunteers. Circulation *116*, 2678–2686. https://doi.org/10.1161/circulationaha.107.724864.

43. Esposito, C.L., Quintavalle, C., Ingenito, F., Rotoli, D., Roscigno, G., Nuzzo, S., Thomas, R., Catuogno, S., de Franciscis, V., and Condorelli, G. (2021). Identification of a novel RNA aptamer that selectively targets breast cancer exosomes. Molecular therapy. Nucleic acids *23*, 982–994. https://doi.org/10.1016/j.omtn.2021.01.012.

44. Lin, C.N., Tsai, Y.C., Hsu, C.C., Liang, Y.L., Wu, Y.Y., Kang, C.Y., Lin, C.H., Hsu, P.H., Lee, G.B., and Hsu, K.F. (2021). An aptamer interacting with heat shock protein 70 shows therapeutic effects and prognostic ability in serous ovarian cancer. Molecular therapy. Nucleic acids *23*, 757–768. https://doi.org/10.1016/j.omtn.2020.12.025.

45. Zhao, S., Tian, R., Wu, J., Liu, S., Wang, Y., Wen, M., Shang, Y., Liu, Q., Li, Y., Guo, Y., et al. (2021). A DNA origami-based aptamer nanoarray for potent and reversible anticoagulation in hemodialysis. Nat. Commun. *12*, 358. https://doi.org/10.1038/s41467-020-20638-7.

46. Chakraborty, S., Dlie, Z.Y., Chakraborty, S., Roy, S., Mukherjee, B., Besra, S.E., Dewanjee, S., Mukherjee, A., Ojha, P.K., Kumar, V., and Sen, R. (2020). Aptamer-functionalized Drug nanocarrier improves hepatocellular carcinoma toward normal by targeting neoplastic hepatocytes. Molecular therapy. Nucleic acids *20*, 34–49. https://doi.org/10.1016/j.omtn.2020.01.034.

47. Yan, A.C., and Levy, M. (2018). Aptamer-mediated delivery and cell-targeting aptamers: room for improvement. Nucleic Acid Ther. *28*, 194–199. https://doi.org/10.1089/nat.2018.0732.

48. He, W., Elizondo-Riojas, M.A., Li, X., Lokesh, G.L.R., Somasunderam, A., Thiviyanathan, V., Volk, D.E., Durland, R.H., Englehardt, J., Cavasotto, C.N., and Gorenstein, D.G. (2012). X-aptamers: a bead-based selection method for random incorporation of druglike moieties onto next-generation aptamers for enhanced binding. Biochemistry *51*, 8321–8323. https://doi.org/10.1021/bi300471d.

49. Bi, J., Yang, L., Wang, T., Zhang, J., Li, T., Ren, Y., Wang, M., Chen, X., Lv, Y., and Wu, R. (2020). Irisin improves autophagy of aged hepatocytes via increasing telomerase activity in liver injury. Oxid. Med. Cell. Longev. *2020*, 6946037. https://doi.org/10.1155/2020/6946037.

50. Zhang, J., Bi, J., Ren, Y., Du, Z., Li, T., Wang, T., Zhang, L., Wang, M., Wei, S., Lv, Y., and Wu, R. (2021). Involvement of GPX4 in irisin's protection against ischemia reperfusion-induced acute kidney injury. J. Cell. Physiol. *236*, 931–945. https://doi.org/10.1002/jcp.29903.

51. Schmidt, J., Rattner, D.W., Lewandrowski, K., Compton, C.C., Mandavilli, U., Knoefel, W.T., and Warshaw, A.L. (1992). A better model of acute pancreatitis for evaluating therapy. Ann. Surg. *215*, 44–56. https://doi.org/10.1097/00000658-199201000-00007.

52. Wang, Z., Wang, H., Mulvenna, N., Sanz-Hernandez, M., Zhang, P., Li, Y., Ma, J., Wang, Y., Matthews, S., Wigneshweraraj, S., and Liu, B. (2021). A bacteriophage DNA mimic protein employs a non-specific strategy to inhibit the bacterial RNA polymerase. Front. Microbiol. *12*, 692512. https://doi.org/10.3389/fmicb.2021.692512.

STAR★METHODS

KEY RESOURCES TABLE

REAGENT or RESOURCE	SOURCE	IDENTIFIER
Antibodies		
Anti-β-Actin	CST	Cat #3700; RRID:AB_2242334
Anti-PDI	CST	Cat #3501; RRID:AB_2156433
Anti-RIP-3	CST	Cat #95702; RRID:AB_2721823
Anti-PINK1	CST	Cat #6946; RRID:AB_11179069
Anti-GRP78	CST	Cat #3183; RRID:AB_10695864
Anti-PGC-1α	Abcam	Cat ab106814
Anti-T-fam	Abcam	Cat ab138351; RRID:AB_2651017
Anti-Mfn-2	Abcam	Cat ab124773; RRID:AB_10999860
Anti-IRE1α	Abcam	Cat ab235171
Anti-p-IRE1α	Abcam	Cat ab48187; RRID:AB_873899
Anti-CIRP	Abcam	Cat ab246510; RRID:AB_2923244
Anti-TLR4	Proteintech	Cat 66350-1-Ig; RRID:AB_2881730
HRP-conjugated Affinipure Goat Anti-Mouse IgG(H+L)	Proteintech	Cat SA00001-1; RRID:AB_2722565
HRP-conjugated Affinipure Goat Anti-Rabbit IgG(H+L)	Proteintech	Cat SA00001-2; RRID:AB_2722564
Anti-Gr1 (LY6G)	Abcam	Cat# ab25377; RRID:AB_470492
Anti-CD11b	Abcam	Cat# ab216445; RRID:AB_2864378
Anti-F4/80	Abcam	Cat# ab240946
Chemicals, peptides, and recombinant proteins		
LPS	Solarbio	Cat#L8880-10mg
Cerulein	Solarbio	Cat#C6660-1mg
Recombinant Cold Inducible RNA Binding Protein (CIRBP)	CLOUD-CLONE	Cat#RPG886Mu01
Hematoxylin and Eosin dye	Servicebio	Cat# G1003
Ham's F-12K	Procell	Cat# PM150910
20% fetal bovine serum	Procell	Cat# 164210-500
Critical commercial assays		
Calcein/PI Cell Viability/Cytotoxicity Assay Kit	Beyotime	Cat# C2015M
Serum amylase assay kit	Nanjing Jiancheng Bioengineering Institute	Cat# C016-1
Serum lipase assay kit	Nanjing Jiancheng Bioengineering Institute	Cat# A054-1
Mouse cold-inducible RNA-binding protein ELISA kit	CUSABIO	CSB-EL005440MO
TNF-α ELISA Kit	CUSABIO	CSB-E04741m
IL-1β ELISA kit	CUSABIO	CSB-E08054m
Experimental models: Cell lines		
Pancreatic AR42J cells	Procell	Cat# CL-0025
Experimental models: Organisms/strains		
C57BL/6 J mice	Experimental Animal Center of Xi'an Jiaotong University	N/A
Software and algorithms		
GraphPad Prism 8	GraphPad Software Inc	https://www.graphpad.com/
ImageJ Software	Open Source	https://imagej.net/software/fiji/

RESOURCE AVAILABILITY

Lead contact

Further information and requests for resources and reagents should be directed to and will be fulfilled by the lead contact, Rongqian Wu (rwu001@mail.xjtu.edu.cn).

Material availability

Antibodies were obtained from the commercial sources described in the STAR Methods key resources table. All material generated in this study are available from the lead contact upon request.

Data and code availability

- All data reported in this paper will be shared by the lead contact upon request.
- This paper does not report original code.
- Any additional information required to reanalyze the data reported in this paper is available from the lead contact upon request.

EXPERIMENTAL MODEL AND STUDY PARTICIPANT DETAILS

Experimental animals and the AP model

Male wild-type C57BL/6 J mice (Experimental Animal Center of Xi'an Jiaotong University, Xi'an, China) and CIRP knockout (KO) mice (Shanghai Model Organisms Center, Inc., Shanghai, China) were used in this study. The CIRP KO mice were generated by deleting CIRP gene on a C57BL/6 J background using the CRISPR/Cas9 technique. The mice were housed in a temperature-controlled room on a 12-h light/dark cycle and fed on a standard laboratory chow diet. The study protocol was approved by the Institutional Animal Care and Use Committee of the Ethics Committee of Xi'an Jiaotong University Health Science Center.

The details of mouse AP model are as follows.[14] The mice (8–10 weeks, 20–22 g) were fasted for 12 h prior to the procedure. AP was induced by two hourly intraperitoneal injections of 4.0 g/kg L-arginine (A0013; Solarbio, beijing, China). The mice were anesthetized with isoflurane inhalation at 72 h after the first injection of L-arginine. Blood and pancreatic samples were collected.

Cell culture

Pancreatic AR42J cells (CL-0025, Procell, Wuhan, China) were cultured in Ham's F-12K (PM150910, Procell, Wuhan, China) with 20% fetal bovine serum (164210-500, Procell, Wuhan, China) in a humidified incubator at 37°C with 5% CO_2. The cells were treated with various concentrations of recombinant CIRP or XA-CIRP as indicated in the figure legends. The living and dead cells were detected using Calcein/PI Cell Viability/Cytotoxicity Assay Kit (C2015M, Beyotime, Shanghai, China) according to the manufacturer's instructions.

METHOD DETAILS

Western blot analysis

The details of Western blot analysis were as follows.[49] The membranes were incubated with primary antibodies at 4°C overnight. Then, the horseradish peroxidase (HRP)-conjugated secondary antibodies were added onto the membranes and incubated at 37°C for 45 min. The bands were displayed by using a digital gel image analysis system (Bio-Rad, United States), and the expression levels of proteins were calculated by ImageJ software. The primary and secondary antibodies used in this study are listed in the key resources table.

Immunohistochemistry

Pancreatic tissue from sacrificed animals was fixed in 4% formalin for paraffin embedding. The primary antibodies against Gr1 (LY6G) (ab25377, Abcam, USA), CD11b (ab216445, Abcam, USA),F4/80 (ab240946, Abcam,USA),TLR4(66350-1-Ig,Proteintech,USA),CIRP(ab246510,Abcam,USA)were used for immunohistochemical staining.[50] The pancreatic paraffin blocks were subjected to dewaxing, soaking, rinsing, antigen retrieval, and serum blocking for 20 min at room temperature. The primary antibodies were incubated with the samples overnight at 4°C, and the secondary antibody for 1 h at room temperature. Then, the samples

were subjected to DAB chromogen, hematoxylin dyeing, alcohol dehydration, clearing and gum sealing. The specific staining of cells in the pancreatic tissue was observed with an optical microscope.

Immunofluorescence

For CIRP immunofluorescence staining, pancreatic tissue samples were fixed with 4% paraformaldehyde and then permeabilized with 0.5% Triton X-100. A primary rabbit anti-CIRP antibody (ab246510,Abcam, USA) was incubated with samples overnight at 4°C. HRP-conjugated Affinipure Goat Anti-Rabbit IgG(H+L) (SA00001-2; Proteintech, USA) was incubated for 1 h at room temperature.

Biochemistry detection

Serum amylase and serum lipase were determined by serum amylase assay kit (C016-1, Nanjing Jiancheng Bioengineering Institute, Nanjing, China) and serum lipase assay kit (A054-1, Nanjing Jiancheng Bioengineering Institute, Nanjing, China) according to the manufacturer's instructions, respectively.

Histologic evaluation of pancreatic injury

Hematoxylin and eosin staining was used to assess pancreatic histology. The pancreatic tissue damage was assessed according to the Schmidt's histological scoring system.[12,51] Scoring criteria details are as follows: Acinar necrosis: Absent(0 point), Focal occurrence of 1-4 necrotic cells/HPF(0.5 point), Diffuse occurrence of 1-4 necrotic cells/HPF(1 point), Same as 1 + focal occurrence of 5-10 necrotic cells/HPF(1.5 points), Diffuse occurrence of 5-10 necrotic cells/HPF(2 points), Same as 2 + focal occurrence of 11-16 necrotic cells/HPF(2.5 points), Diffuse occurrence of 1 1-16 necrotic cells/HPF (foci of confluent necrosis) (3 points), Same as 3 + focal occurrence of > 16 necrotic cells/HPF(3.5 points) , > 16 necrotic cells/HPF (Extensive confluent necrosis) (4 points).

Transmission electron microscopy (TEM)

Seventy nm ultra-thin sections of pancreatic tissue samples were stained with uranyl acetate and lead citrate. For transmission electron microscope, about 1 mm^3 pancreas tissues were fixed in 2.5% glutaraldehyde. Pancreas tissues were prefixed after harvesting immediately with 1.5% glutaraldehyde and 0.8% paraformaldehyde (0.1 mol/L cacodylate buffer) at room temperature and postfixed in an aqueous solution of 1% OsO4 and 1.5% $K_4(FeCN)_6$. Then the specimens were embedded into Epon by routine procedures. Three fields were randomly selected under electron microscope for application. Pancreatic ultrastructure were evaluated using a transmission electron microscope (HT7700, Hitachi, Japan) by a single electron microscopist.

Enzyme-linked immunosorbent assay (ELISA)

Mouse cold-inducible RNA-binding protein ELISA kit (CSB-EL005440MO, CUSABIO, Wuhan, China), TNF-α ELISA Kit (CSB-E04741m, CUSABIO, Wuhan, China) and IL-1β ELISA kit (CSB-E08054m, CUSABIO, Wuhan, China) were used to evaluate the levels of CIRP, TNF-α and IL-1β in serum samples.

Selection and synthesis of X-Aptamers

CIRP targeting X-Aptamers were identified in a bead-based selection process using the X-Aptamer selection kit from AM Biotechnologies (Houston, TX, USA). The recombinant human CIRP protein (APG886Hu01, Cloud-Clone Corp, Wuhan, China) was used as the target molecule. Detailed selection protocol: X-Aptamer oligonucleotides that bound to human CIRP protein were enriched and isolated according to the X-Aptamer selection protocol.[9] The selected X-Aptamer oligonucleotides were amplified into unmodified oligonucleotides by PCR. The PCR products were subjected to next-generation sequencing (Ion Torrent PGM, Life Technologies). The sequencing data were analyzed by AM Biotechnologies. Sequences with a high frequency of occurrence in selection fractions containing the protein targets when compared to protocol controls were identified as X-Aptamer candidates (supplemental information:Figure S5). These X-Aptamer candidates were resynthesized as oligonucleotides consisting of a 42 nt random region, 5 additional T's on the 5′-end and CCATG on the 3′-end by AM Biotechnologies.

NMR structure determination

The structural determination of CIRP was performed in a high salt buffer (300 mM NaCl, 50 mM K_2HPO_4, 1mM TCEP, pH 6.5). NMR spectra were collected at 300K from Bruker 600MHz (Avance III) spectrometer equipped with cryo-probes. Spectral assignments were completed using our in-house, semi-automated

assignment algorithms and standard triple-resonance assignment methodology. NMR titrations were performed in a buffer (300 mM NaCl, 50 mM KH_2PO_4, 0.2 mM TCEP, pH 6.5). Unlabeled ssRNA or the extracellular domain of TLR4 were added to ^{15}N-labeled CIRP (0.5 mM), according to stoichiometric ratio indicated to perform NMR titration. The peaks experienced most peak broadening effect (ratio< 0.1) are labeled.[52]

Isothermal titration calorimetry (ITC)

ITC experiments were performed on a MicroCal PEAQ-ITC Instrument (Microcal) at 25°C using the dialysis buffer described above. Briefly, 60 μM Aptamer or 200 μM of TLR4 in the cell was titrated with 0.5 mM CIRP in the syringe via 19 injections with 2 μL each at 120 s interval. The raw data were integrated, normalized for the molar concentration and analyzed using MicroCal PEAQ-ITC Analysis Software.

Administration of XA-CIRP in AP mice

To investigate the therapeutic effects of XA-CIRP in AP mice, XA-CIRP (10 nmol/kg BW) or control was administered via the tail vein 2 h after the second injection of L-arginine solution in male adult C57BL/6 J mice. Blood and pancreatic tissue samples were harvested at 72 h after the first injection of L-arginine (i.e., 69 h after the injection of XA-CIRP). The dose of XA-CIRP was chosen based on a previous study in which the authors used microRNA 130b-3p to block extracellular CIRP-induced inflammation.[11]

QUANTIFICATION AND STATISTICAL ANALYSIS

The data in this paper were expressed as means ± standard error and analyzed using GraphPad Prism 8 Software. The *t*-test or one-way ANOVA with the Student-Newman-Keuls test was used to analyze the differences between groups. $P < 0.05$ indicates a statistically significant difference.